



Research Article

Adsorption of Chromium(VI) onto Freshwater Snail Shell-Derived Biosorbent from Aqueous Solutions: Equilibrium, Kinetics, and Thermodynamics

Xuan Hoa Vu,¹ Lan Huong Nguyen,² Huu Tap Van ,³ Dinh Vinh Nguyen,⁴ Thu Huong Nguyen,³ Quang Trung Nguyen,³ and L. T. Ha ^{5,6}

¹Institute of Research and Development, Duy Tan University, Da Nang 550000, Vietnam

²Faculty of Environment—Natural Resources and Climate Change, Ho Chi Minh City University of Food Industry (HUPI), 140 Le Trong Tan Street, Tay Thanh Ward, Tan Phu District, Ho Chi Minh City, Vietnam

³Faculty of Natural Resources and Environment, Thai Nguyen University of Sciences (TNUS), Tan Thinh Ward, Thai Nguyen, Vietnam

⁴Faculty of Chemistry, Thai Nguyen University of Sciences (TNUS), Tan Thinh Ward, Thai Nguyen, Vietnam

⁵Ceramics and Biomaterials Research Group, Advanced Institute of Materials Science, Ton Duc Thang University, Ho Chi Minh City, Vietnam

⁶Faculty of Applied Sciences, Ton Duc Thang University, Ho Chi Minh City, Vietnam

Correspondence should be addressed to L. T. Ha; letienha@tdtu.edu.vn

Received 15 June 2019; Revised 26 July 2019; Accepted 30 July 2019; Published 22 September 2019

Academic Editor: Cláudia G. Silva

Copyright © 2019 Xuan Hoa Vu et al. This is an open access article distributed under the Creative Commons Attribution License, which permits unrestricted use, distribution, and reproduction in any medium, provided the original work is properly cited.

In this study, freshwater snail shells (FSSs) containing CaCO₃ were used as a low-cost biosorbent for removing Cr(VI) from aqueous solutions. The characteristics of FSS and mechanism of Cr(VI) adsorption onto FSS were investigated. The FSS biosorbent was characterized using nitrogen adsorption/desorption isotherm, X-ray diffraction, scanning electron microscopy with energy dispersive spectroscopy, and Fourier transform infrared spectroscopy. The adsorption mechanism was determined by conducting various batch adsorption experiments along with fitting experimental data with various adsorption models. Batch adsorption experiments were conducted as a function of solution pH, contact time, biosorbent dose, and initial Cr(VI) concentration. Results indicated that pH = 2, a contact time of 120 min, and an initial Cr(VI) concentration of 30 mg/L at 20°C were the best conditions for adsorption of Cr(VI) onto FSS. The Cr(VI) adsorption onto FSS decreased with an increase in temperature from 20 to 40°C. The obtained maximum adsorption capacity was 8.85 mg/g for 2 g/L of FSS dose with 30 mg/L of initial Cr(VI) at 20°C. The adsorption equilibrium data fit well with the Sips and Langmuir isotherm models at 20°C with a high R² of 0.981 and 0.975, respectively. Also, a good correlation between the experimental data and the pseudo-second-order model was achieved, with the highest R² of 0.995 at 20°C. The adsorption mechanisms were electrostatic interaction and ion exchange. Simultaneously, this mechanism was also controlled by film diffusion. The Cr(VI) adsorption process was irreversible, spontaneous (−G°), exothermic (H° is negative), and less random (S° is negative). In conclusion, freshwater snail shells have the potential as a renewable adsorbent to remove toxic metals from wastewater.

1. Introduction

Chromium is a highly toxic agent to humans and other living organisms, which is discharged into receiving sources from many industrial activities, including leather tanning, electroplating, metal processing, dyeing, chromate preparation,

and leathers [1]. In aqueous solutions, chromium exists in both trivalent (Cr(III)) and hexavalent (Cr(VI)) forms [2–5]. Compared with Cr(III), Cr(VI) is more mobile, hard to treat, and about 10–100 times more toxic [1, 6]. Cr(VI) may cause lung cancer [3], epigastric pain, severe diarrhea, hemorrhage, dermatitis [4], tissue necrosis, and skin irritation [1].

For many decades, several techniques, such as reverse osmosis and direct precipitation [1], electrochemical reduction, ion exchange [7], biological treatment [8, 9], coagulation, solvent extraction, membrane separation, biosorption [10–12], artificial radiation, and solar radiation in a tubular reactor, are being followed to remove Cr(VI) from polluted waters [13]. Among these methods, adsorption has been acknowledged to be the most economically favorable method due to its low energy consumption and high efficiency, even at a very low Cr(VI) concentration.

Biosorbents are adsorbents derived from various kinds of biomass, mainly industrial and agricultural by-products, such as clay, corncob, and fly ash [2, 14, 15], which are used for the removal of various contaminants from the water environment. Among them, a large number of low-cost biosorbents developed from different by-products, such as tamarind nut carbon [12], green coconut shell [3], sugarcane bagasse [4], coffee husk [5], rice husk [16], waste fruit cortexes [17], and mango kernel [18], had been used for aqueous Cr(VI) adsorption. Especially, the materials containing biogenic calcium carbonate (CaCO_3) have been attracting much attention from scholars. Such composite biomaterials showed high affinity to many harmful trace metals, such as Pb, Cd, Cr, Ni, and Zn, in solution. Thus, these biomaterials are used to develop CaCO_3 -rich materials for preparing low-cost adsorbents. For instance, Flores-Cano et al. [19] developed an eggshell-derived biosorbent for Cd adsorption; El Haddad [20] used a calcined mussel shell (62.24% CaCO_3)-derived biosorbent to remove Basic Fuchsin dye; Van et al. [21] developed a green biosorbent derived from freshwater mussel shells (contain >90% CaCO_3) for the removal of Cd with an adsorption capacity of 26.6 mg/g.

Fresh snail is one of the popular foods in Vietnam and Asia. The freshwater snail shell (FSS) waste directly discharged into environment causes foul odor, affecting human health and aesthetics. However, fresh snail shell is a CaCO_3 -rich material and is a potential feedstock for biosorbent preparation with economic and environmental significances. As a biosorbent, FSS offers promising advantages, including large surface area, high porosity, small foam density, and good chemical resistance. Hence, FSS can potentially serve as a green biosorbent to remove trace metals such as Cr(VI) from aqueous solutions. The aim of this study, therefore, was to develop an inexpensive biosorbent from FSS for the removal of toxic Cr(VI) from aqueous solutions. Characteristics of FSS, adsorption isotherm, kinetics, and mechanism of Cr(VI) onto FSS were thoroughly investigated through batch experiments under various operational conditions.

2. Materials and Methods

2.1. Preparation of Biosorbent. The fresh snail shell (FSS) wastes were collected from local restaurants in Thai Nguyen, Vietnam. The FSSs were cleaned three times with tap water and air-dried under sunlight. The dried FSSs were then soaked in 0.1 M sulfuric acid solution to remove soluble matter on their surface and repeatedly washed with distilled water to remove residual acid until the solution pH was constant. After drying at 80°C for 24 h, the FSSs were ground and sieved to

obtain particles ≤ 0.5 mm in size. The obtained FSS powder was then stored in plastic containers for further usage.

2.2. Characteristics of Biosorbent. The surface area (S_{BET}) of FSS was determined by nitrogen adsorption/desorption isotherm at 77.350 K (Coulter, USA). The morphology of FSS was analyzed using scanning electron microscopy (SEM, Hitachi S-4800). The FSS crystal structure was characterized using an X-ray diffractometer (D8 ADVANCE) equipped with a copper tube by scanning 2θ from 10° to 80° with a 2°/min rate ($\lambda_{\text{K}\alpha} = 0.15418$ nm). The presence of surface functional groups was detected using Fourier transform infrared spectroscopy (FT/IR-6300) with wavenumbers from 4000 to 500 cm^{-1} .

pH_{PZC} was determined according to the pH shift method [22]: first, 10 mL of 0.01 M NaCl solutions were adjusted to a desirable pH value ($\text{pH}_{\text{initial}}$; from 3 to 10) with 0.1 M NaOH and 0.1 M H_2SO_4 . Then, 30 mg of FSS was added to the NaCl solution in a 100 mL Erlenmeyer flask and shaken on a shaker for 48 h at 120 rpm at room temperature ($25 \pm 1^\circ\text{C}$). The suspended solution was decanted and the final pH (pH_{final}) was measured. The difference between $\text{pH}_{\text{initial}}$ and pH_{final} was pH , which was further plotted against $\text{pH}_{\text{initial}}$. The pH_{PZC} value was calculated for $\text{pH} = 0$ using a cubic spline interpolation method.

2.3. Batch Experiment of Cr(VI) Adsorption onto FSS. The chemicals used were $\text{K}_2\text{Cr}_2\text{O}_7$, H_2SO_4 , and NaOH (purchased from Merck, Germany). Cr(VI) stock solution (1000 mg/L) was prepared by accurately dissolving 2.8287 g $\text{K}_2\text{Cr}_2\text{O}_7$ in 1000 mL deionized water. Desirable concentrations of Cr(VI) solution in range between 5 mg/L, 10 mg/L, 20 mg/L, 30 mg/L, 40 mg/L, 50 mg/L, 60 mg/L, 70 mg/L, and 80 mg/L were prepared by diluting the above stock solution with deionized water.

Each adsorption experiment was carried out by mixing a definite amount of FSS with 25 mL of Cr(VI) solution in an Erlenmeyer flask. The pH of the mixture was adjusted using 1 M H_2SO_4 or 1 M NaOH solution. The mixture was shaken at 120 rpm at a definite temperature in a proper time. Then, the mixture was filtered by using a Whatman No. 1 filter paper (pore size of 11 μm). The concentration of Cr(VI) in the filtrate was analyzed by Atomic Absorption Spectrometry (AAS, Hitachi Z 2000). The experiments were conducted to investigate effects of various parameters on Cr(VI) adsorption onto FSS, namely, solution pH (2.0–9.0), contact time (20–180 min), initial Cr(VI) concentration (30–200 mg/L), and biosorbent dosage (2–30 g/L) and temperature (20–40°C).

The amounts of Cr(VI) adsorbed onto the biosorbent at equilibrium (q_e ; mg/g) and any time t (q_t ; mg/g) were calculated according to the following equation:

$$q_e = \frac{(C_0 - C_e)V}{W},$$

$$q_t = \frac{(C_0 - C_t)V}{W},$$
(1)

where C_0 (mg/L), C_t (mg/L), and C_e (mg/L) are Cr(VI) concentrations at the initial time ($t=0$), any time t , and equilibrium, respectively; V (L) is the working volume of Cr(VI) solution; and W (g) is the weight of used biosorbent.

3. Results and Discussion

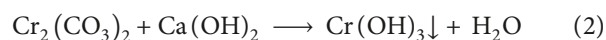
3.1. Characteristics of Biosorbent. The obtained results of nitrogen adsorption/desorption isotherm indicated that FSS is a nonporous material because of its poor textural properties with the total pore volume of $<0.001 \text{ cm}^3/\text{g}$ and the BET area (S_{BET}) of $<2 \text{ m}^2/\text{g}$. This implied S_{BET} was not the main factor effecting the Cr(VI) adsorption onto FSS and suggested that the contribution of pore filling in the adsorption mechanism of Cr(VI) onto FSS is negligible. The surface morphology of FSS was observed using a scanning electron microscopy and the results are presented in Figure 1. The SEM image reveals that FSS has a rough and lamellar surface, and a nonporous structure with defined channels/cavities and many trenches. The rod-shaped FSS particles had many crystalline micro-layers and their thickness and width, respectively, were $1.5 \mu\text{m}$ and $2.8 \mu\text{m}$. This result agreed with several previous reports by Van et al. [21] with S_{BET} of $1.45 \text{ m}^2/\text{g}$ for a CaCO_3 -rich biosorbent—biogenic aragonite shells—and $2.09 \text{ m}^2/\text{g}$ for golden apple snail shells [22].

Figure 2 describes the XRD spectrum of FSS. The XRD pattern of FSS has the diffraction lines at 2 theta angles of 26.4, 27.59, 31.42, 33.47, 36.43, 38.14, 38.71, 41.31, 43.05, 46.02, 48.53, 50.36, 52.63, and 53.1° corresponding to the reflection of planes (111), (021), (104), (002), (012), (102), (031), (022), (122), (221), (202), (132), (113), and (032), respectively, in the orthorhombic structure of aragonite (JCPDS 05-0453), CaCO_3 . In addition, the characteristic peaks of calcium silicate (Ca_2SiO_4) were also observed with low intensity on the XRD pattern, indicating the small amount of this compound present in FSS. The high intensity and the intensive sharpness of the aragonite diffraction lines imply the high crystallinity and the dominance of aragonite, suggesting that FSS is a nearly pure biogenic aragonite (98% CaCO_3). This result is similar to the findings reported in [23, 24] about the presence of aragonites as constituents of the *Pinctada martensii* pearls and the shells of the mollusc *Pinctada maxima*.

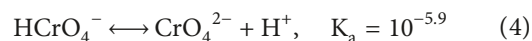
Additionally, Figure 3 illustrates the FTIR results of FSS. The results reveal the presence of dominant functional groups on the FSS surface. The adsorption spectrum wavenumbers varied from 450 to 4000 cm^{-1} . The presence of CO_3^{2-} polymorph adsorption groups was detected by the bands at wavenumbers of 699, 712, 862, 1082 and 1471 cm^{-1} . The occurrence of C=O groups of the carbonate ions on the FSS surface corresponds to the band at the wavenumber of 1787 cm^{-1} . The vibration of C-H bonds occurred at the bands at 2852 and 2918 cm^{-1} . The peaks found at 2498, 2523, 2547, and 3396 cm^{-1} can be assigned for the OH group of carboxylic acids. Lim and Aris [25] pointed out that the carbonyl (C=O) group appearing in eggshells and coral wastes functioned as an active group for complexation with toxic metal ions (i.e., Pb^{2+} , Cd^{2+} , and Cu^{2+}). XRD and FTIR

clearly confirmed the existence of CaCO_3 as a major component in the FSS structure.

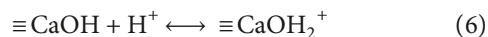
3.2. Effect of pH. Figure 4(a) presents the effect of pH on the adsorption capacity of Cr(VI) onto FSS. Obviously, the adsorption process strongly depended on the solution pH. Namely, the Cr(VI) adsorption capacity onto FSS decreased from 44.12 mg/g to 0.72 mg/g with an increase in solution pH from 2 to 9. The maximum adsorption capacity, therefore, was obtained at pH 2. Figure 4(b) indicated higher pH_{PZC} than the others that might result from the presence of CaCO_3 . According to pH_{PZC} , the surface of FSS was positively charged in the pH from 2.0 to 9.0 due to $\text{pH}_{\text{PZC}} > \text{pH}_{\text{solution}}$. At acid pH, the adsorption capacity of Cr(VI) onto FSS can be explained as: Cr(VI) was first reduced to Cr(III), then Cr(III) combined with OH^- group on the FSS surface according to the following reaction:



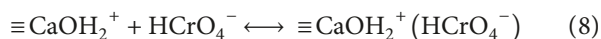
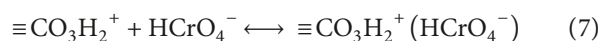
Besides, the dependence of the adsorption capacity of Cr(VI) onto FSS on pH can be explained by the effect of functional groups on the FSS surface. Two kinds of functional groups, $\equiv\text{CO}_3\text{H}$ and $\equiv\text{CaOH}$ on the FSS surface, interact with species of Cr(VI) in aqueous solutions. Cr(VI) exists in various stable forms, including CrO_4^{2-} , HCrO_4^- , and $\text{Cr}_2\text{O}_7^{2-}$ [25] depending on pH. The different species of Cr(VI) in aqueous solutions are given by the following equilibrium equations:



At solution pH 2, the dominant form of Cr(VI) is HCrO_4^- and at higher pH the dominant form of chromium is CrO_4^{2-} [18]. At a low pH value, the functional groups are protonated and become the positive forms. In this case, the adsorption of Cr(VI) onto FSS is strongly dependent on the positive charge on the surface of the adsorbent as follows:



And, the adsorption reactions could be rewritten as:



Although CrO_4^{2-} is dominant at a high pH value, the positive charge decreases, leading to the decrease in adsorption.

Therefore, at lower pH, the attraction between HCrO_4^- and the adsorbent was enhanced, leading to an increase in the adsorption capacity due to an increase in the number of protons on the surface of the adsorbate [26]. At a higher pH value (alkaline environment), Cr(VI) mainly exists in the form of CrO_4^{2-} [26] and the concentration of the OH^- ions increase. Consequently, the competition between the OH^-

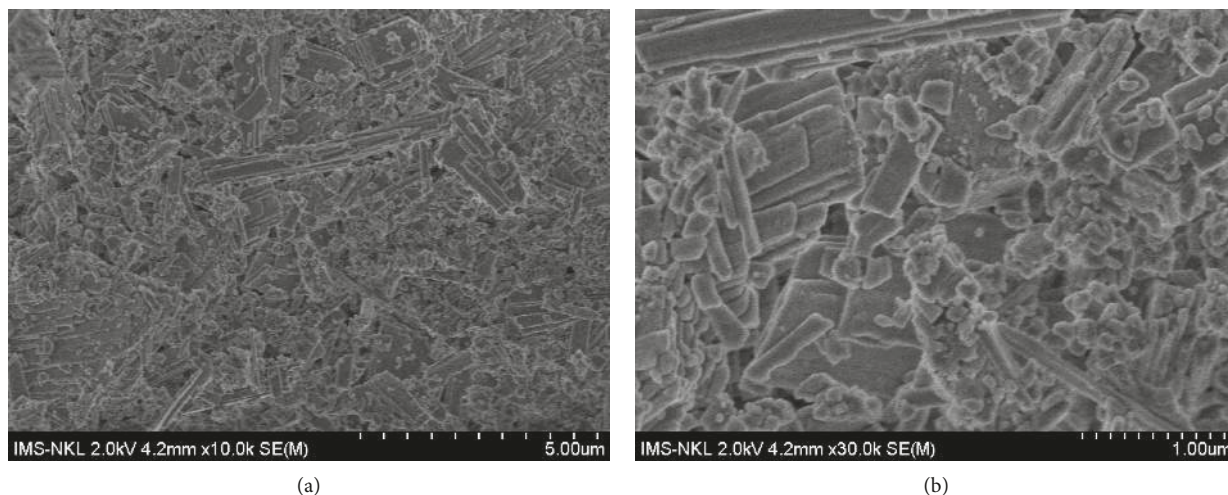


FIGURE 1: SEM images of FSS.

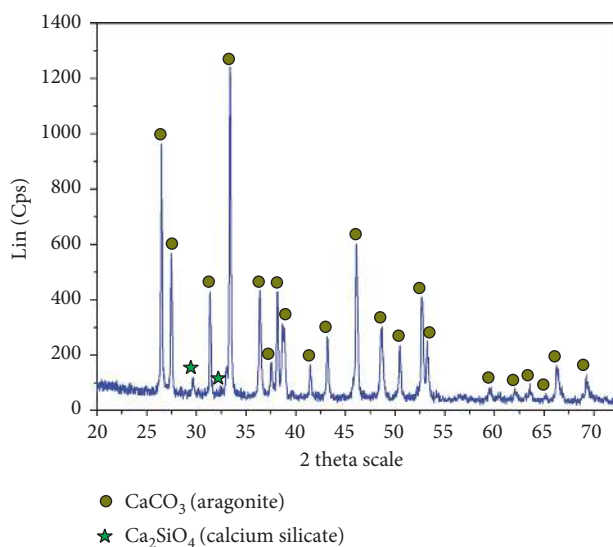


FIGURE 2: XRD pattern of FSS.

and Cr(VI) anions occurs causing an interaction between OH^- and the functional groups on the FSS surface leading to a decrease in the Cr(VI) adsorption capacity onto FSS. The high adsorption capacity of Cr(VI) at the low pH value could be assigned to electrostatic attraction and/or by the binding of HCrO_4^- to acidic functional groups on FSS's surface [27, 28]. As a result, pH 2 is the optimum value for adsorption of Cr(VI) onto FSS. This finding is very consistent with the results reported by Rai et al. [18] and Owalude et al. [29] who showed similar trends for hexavalent chromium adsorption as a function of pH.

3.3. Effect of Initial Cr(VI) Concentration and Adsorption Isotherms. To study the effect of initial Cr(VI) concentration on the adsorption capacity, the experiments were carried out with varying initial Cr(VI) concentrations ranging from 30 to 200 mg/L at various temperatures from 20 to 40°C. The obtained results are presented in Figure 5. It can be clearly seen

from Figure 5 that when increasing initial concentrations of Cr(VI) and decreasing temperature, the amount of Cr(VI) adsorbed onto FSS significantly increased as follows: 4.33–8.87 mg/g at 20°C; >3.17–8.14 mg/g at 30°C; and >2.63–7.65 mg/g at 40°C. The decrease in the adsorption capacity shows that low temperature favors Cr(VI) adsorption onto FSS. In this study, the highest adsorption capacity was 8.81 and 8.87 mg/g at 20°C with initial Cr(VI) concentrations of 150 and 200 mg/L, respectively. According to Sdiri et al. [30], the rising temperature resulted in dissolving more calcite and releasing more bicarbonate ions into solution. Consequently, competition between HCO_3^- and HCrO_4^- occurred under acidic conditions, which led to a decrease in Cr(VI) adsorption capacity. Besides, higher temperature accelerates the mobility of the ions and desorption of HCrO_4^- [26]. The weakening of supportive forces between the active sites on the adsorbent and the destruction of active binding sites at higher temperature leads to the decrease in adsorption capacity [30, 31]. A similar trend was reported by Akram et al. [27] about adsorption of Cr(VI) onto biocomposite of mango (*Mangifera indica*).

In order to elucidate the adsorption mechanism of Cr(VI) onto FSS, three isotherm models were fitted to the obtained experimental data: Langmuir, Freundlich, and Sips.

The applicability of the models was evaluated by the correlation coefficient (R^2). The Langmuir model [32, 33] is expressed as follows:

$$q_e = \frac{q_m \cdot b \cdot C_e}{1 + bC_e}, \quad (9)$$

where C_e is the equilibrium concentration in liquid phase (mg/L), q_m is the maximum adsorption capacity (mg/g), and b is the Langmuir constant related to the free adsorption energy (L/mg).

The fundamental characteristics of the Langmuir isotherm are expressed by a dimensionless separation factor, R_L , described as follows:

$$R_L = \frac{1}{1 + q_m b C_{0(\max)}}, \quad (10)$$

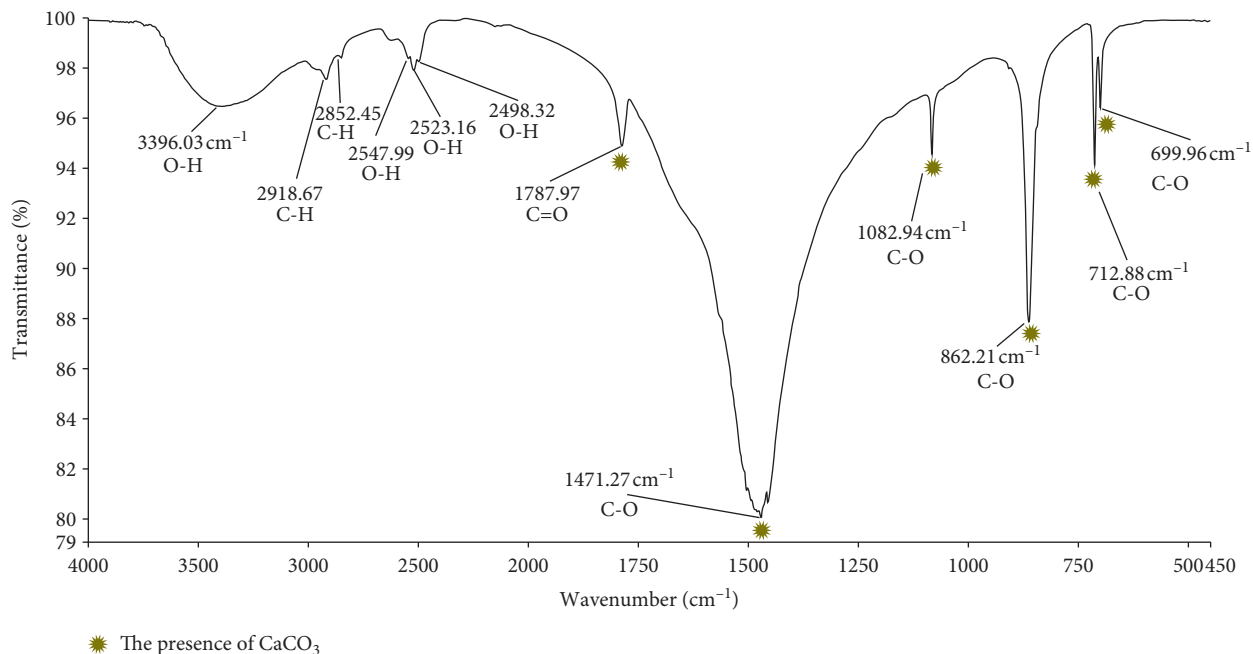
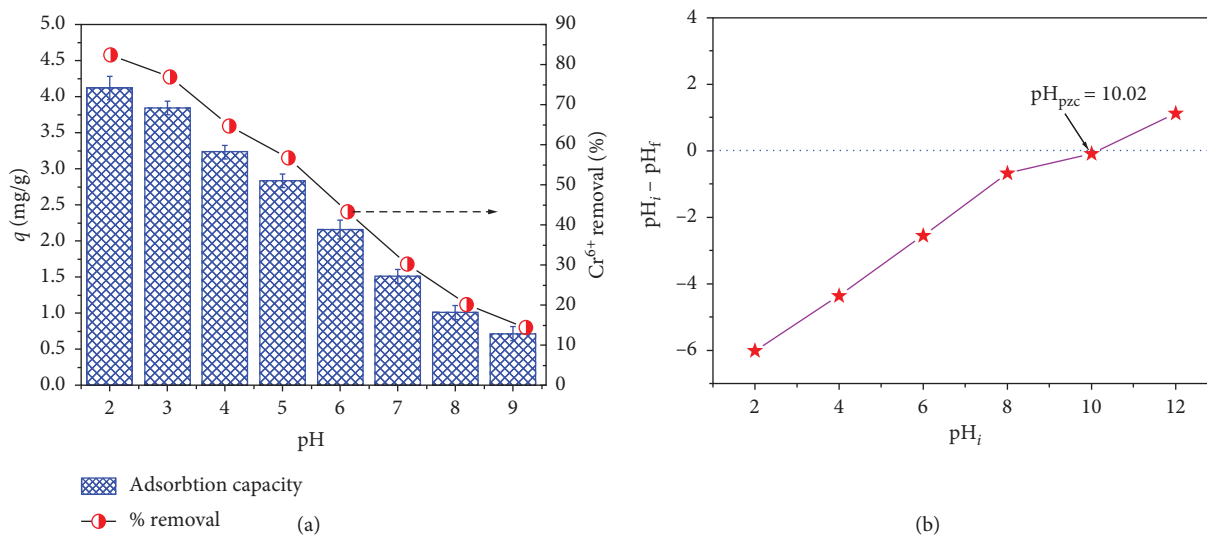


FIGURE 3: FTIR spectrum of FSS.

FIGURE 4: (a) Effect of solution pH on Cr(VI) adsorption by FSS at 10 mg/L of initial Cr(VI); 4 g/L of adsorbent dosage; 20°C; 120 min of contact time; (b) pH_{PZC} of FSS.

where C_0 (max) is expressed as the highest initial adsorbate concentration. The R_L parameter indicates the shape of isotherm, namely, $R_L > 1$, unfavorable; $0 < R_L < 1$, favorable; $R_L = 0$, irreversible. The Freundlich model [32, 34] is:

$$q_e = K_F C_e^{1/n}, \quad (11)$$

where K_F is a constant indicative of the adsorption capacity of the adsorbent ($\text{mg}(1^{-1/n})\text{L}(1/n)/\text{g}$) and constant $1/n$ refers to the intensity of the adsorption.

The Sips model is a combination of both the Langmuir and Freundlich isotherm models. The equation below describes the Sips isotherm model:

$$q_e = \frac{q_m (bC_e)^{1/n}}{1 + (bC_e)^{1/n}}. \quad (12)$$

The parameters of the three models were evaluated by nonlinear regression analysis using Origin 9.0 software, and the results are given in Table 1.

According to Table 1, the value of separation factor (K_L) of the Langmuir model fell between 0 and 1. The value of the exponent (n_F) from the Freundlich isotherm was between 1 and 10, which proved that the conducted adsorption processes were favorable at temperatures from 20 to 40°C. The Sips isotherm constant (n) changed from

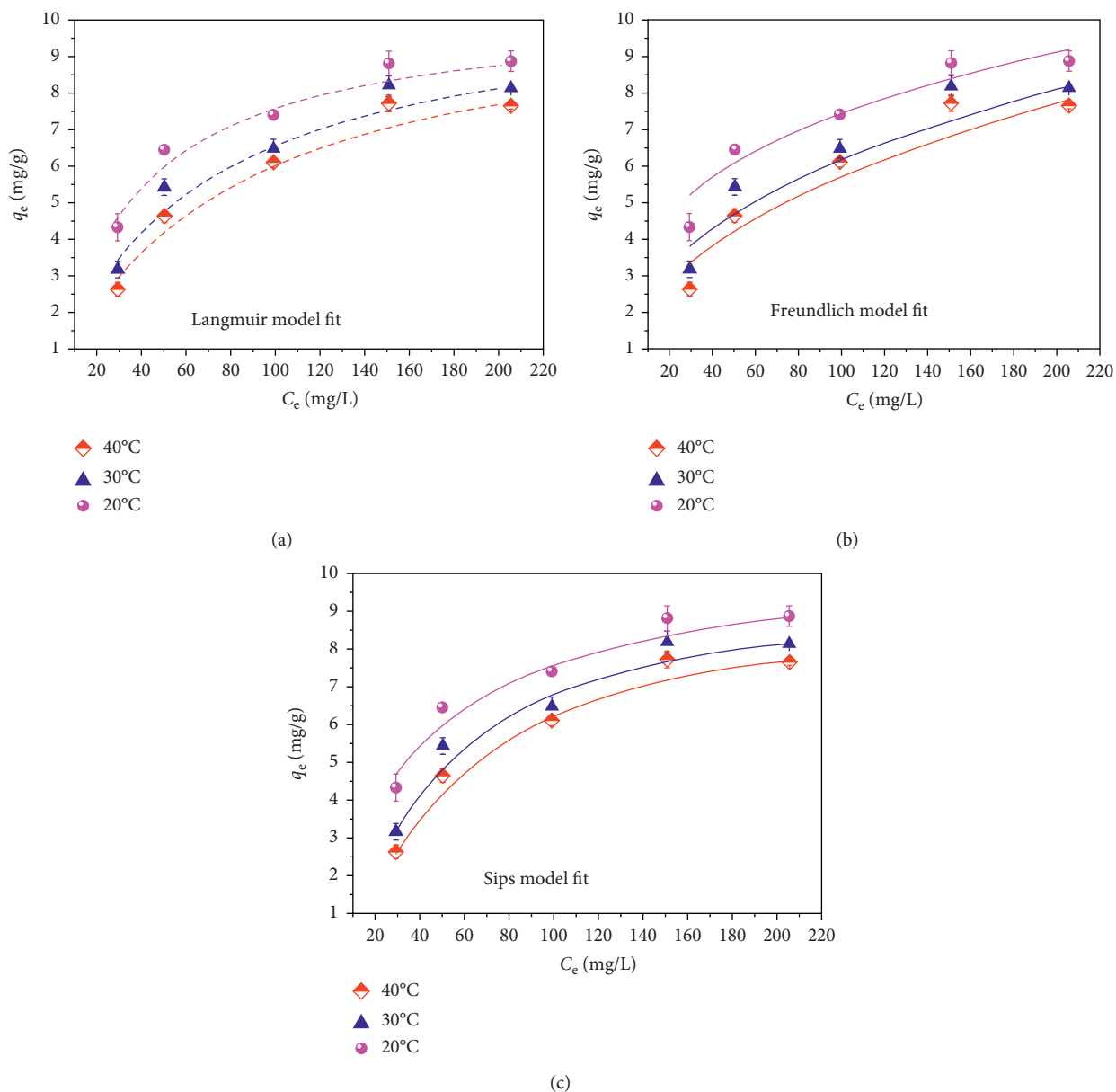


FIGURE 5: Effect of initial Cr(VI) concentration on Cr(VI) adsorption onto FSS at various temperatures; pH 2; 120 min of contact time; 4 g/L of adsorbent dosage.

0.910 to 1.415 with an increase in temperature from 20 to 40°C, which implied that the surface of FSS was heterogeneous in nature. The correlation coefficients (R^2) of Langmuir and Sips models were closer to unity in comparison to the Freundlich model, indicating that adsorption data are fitted well to this model at temperatures from 20 to 40°C. The maximum adsorption capacity calculated from Langmuir and Sips models was 10.69 and 10.82 mg/g at 20°C, respectively, very close to the equilibrium experimental value of 8.81 mg/g, which also confirmed the good agreement between the obtained experimental data and the Sips model. Similar findings have been reported for Cr(VI) adsorption onto different biomasses such as maize corncob [35], sugarcane bagasse [36], and *Swietenia mahagoni* [37].

3.4. Effect of Contact Time and Adsorption Kinetics. The effect of contact time on the adsorption of Cr(VI) onto FSS was conducted with varying contact time from 5 to 180 min at pH 2, adsorbent dose of 4 g/L, and initial Cr(VI) concentration of 30 mg/L. All experiments were performed in flasks shaken at 120 rpm agitation and temperature from 20 to 40°C. Figure 6 presented the obtained results. Clearly, at the beginning of the process, the Cr(VI) adsorbed onto FSS significantly increased until almost 60 min. By further increasing the contact time, the adsorbed amount increased slowly and remained unchanged after 120 min at all studied temperature ranges. It can be explained that there was an interactive force between solute molecules in the solid phase (FSS) and bulk phase leading to an occupation of the vacant active sites on the biosorbent surface. And, the adsorption and desorption process tend to

TABLE 1: The calculated isotherm parameters of Langmuir, Freundlich, and Sips models for Cr(VI) adsorption on FSS at various temperatures.

	Unit	Temperature		
		20°C	30°C	40°C
Langmuir model				
Q_{\max}°	mg/g	10.69	10.61	10.38
K_L	L/mg	0.275	0.164	0.131
R^2	—	0.975	0.983	0.969
Freundlich model				
K_F	(mg/g)(mg/L) ⁿ	0.762	1.012	1.948
n_F	—	2.286	2.548	3.435
R^2	—	0.922	0.946	0.941
Sips model				
Q_{\max}°	mg/g	10.82	9.29	8.91
b	—	0.013	0.021	0.018
n	—	0.910	1.350	1.415
R^2	—	0.951	0.984	0.981

be equal with longer residence time. Therefore, the adsorption rate was lower when the contact time was further increased [38]. Figure 6 indicated the adsorption of Cr(VI) onto FSS reached equilibrium after 120 min. The adsorbed amount at equilibrium reached 6.64, 6.23, and 5.51 mg/g corresponding to a temperature of 20, 30, and 40°C, respectively. Similar trend of chromium adsorption has also been presented previously for different adsorbents such as activated carbon derived from wood apple shell [39], magnetic multiwall carbon nanotubes [40], and magnetic nanocomposites [41].

In order to analyze the adsorption kinetics of Cr(VI) onto FSS several models were fitted to the experimental data, namely, pseudo-first-order, pseudo-second-order, and Elovich models.

The pseudo-first-order model is presented as follows:

$$q = q_e(1 - e^{-k_1 t}), \quad (13)$$

where k_1 (1/min) is the adsorption rate constant of the model.

The pseudo-second-order model is given as follows:

$$q = \frac{q_e^2 k_2 t}{1 + q_e k_2 t}, \quad (14)$$

where k_2 (g/mg.min) is the second-order adsorption rate constant.

The Elovich model is expressed as follows:

$$q = \frac{1}{\beta} \ln(\alpha \beta t), \quad (15)$$

where α (mg/g.min) is the initial sorption rate and β (g/mg) is the constant related to the extent of surface coverage and activation energy of chemisorption in the Elovich model.

All the calculated parameters of the three models are presented in Table 2.

Generally, the correlation coefficient (R^2) of all selected models was near unity, implying that the adsorption process can be well described by these models. However, q_e (6.78 mg/g at 20°C) calculated from the pseudo-second-order model was the closest to experimental data (6.64 mg/g) with a highest

correlation coefficient of $R^2 = 0.995$. This indicated that the pseudo-second-order model is the most proper one to describe the adsorption mechanism of Cr(VI) onto FSS [26, 42].

To further understand the controlling step of the adsorption rate, the experimental data were fitted to the intraparticle diffusion model, expressed as follows:

$$q = k_i t^{0.5}, \quad (16)$$

where k_i (mg/g.min) is the intraparticle diffusion rate constant calculated from the slope of the plot q versus $t^{0.5}$ (Figure 7).

It can be seen from Figure 7 that there were three linear plots in each of the three different temperatures. This indicates that the Cr(VI) adsorption process was controlled by multiple steps, including bulk diffusion, intraparticle diffusion, and adsorption at active sites. The results of deviation of plot using Origin 9.0 software might result from the difference in rate of mass transfer at the initial and final stages of the adsorption process. The calculated intercepts indicated that the adsorption process was controlled by film diffusion while the intraparticle diffusion had a negligible effect.

3.5. Effect of Adsorbent Dosage. The various dosages of FSS (2, 4, 6, 8, 10, 12, 14, 16, 18, 20, 22, 24, 26, 28, and 30 g/L) in 30 mg/L of initial Cr(VI) were studied for Cr(VI) adsorption at optimum pH (pH 2) and a contact time of 120 min. The results are presented in Figure 8. It can be seen from Figure 8 that the adsorption percentage of Cr(VI) onto FSS increased significantly from 25.29% to 41.86%, which corresponded with an increase in doses of FSS in range from 2 to 10 g/L. The explanation for this may be due to the increase in biosorbent dosage resulting in the increase in number of active sites on the FSS surface. Consequently, more Cr(VI) ions were attached to the active sites on the FSS surface. However, the Cr(VI) removal efficiency did not increase when increasing the amount of FSS due to a limitation of active sites for Cr(VI). The result was due to a full saturation of the adsorption process [43, 44]. The adsorption capacity declined from 8.85 mg/g to 0.95 mg/g in accordance with an increase in the adsorbent dosage from 2 to 30 g/L. The maximum adsorption capacity (8.85 mg/g) was achieved at the dosage of 2 g/L with 30 mg/L of initial Cr(VI).

3.6. Adsorption Thermodynamics. The mechanism of adsorption can be investigated according to thermodynamic parameters such as change in Gibbs free energy (ΔG°), change in enthalpy of adsorption (ΔH°), and change in entropy (ΔS°) [40]. These parameters were estimated by the Van't Hoff equation as follows:

$$\Delta G^{\circ} = -RT \ln K,$$

$$\Delta G^{\circ} = \Delta H^{\circ} - T\Delta S^{\circ}, \quad (17)$$

$$\ln K = -\frac{\Delta H^{\circ}}{RT} + \frac{\Delta S^{\circ}}{R},$$

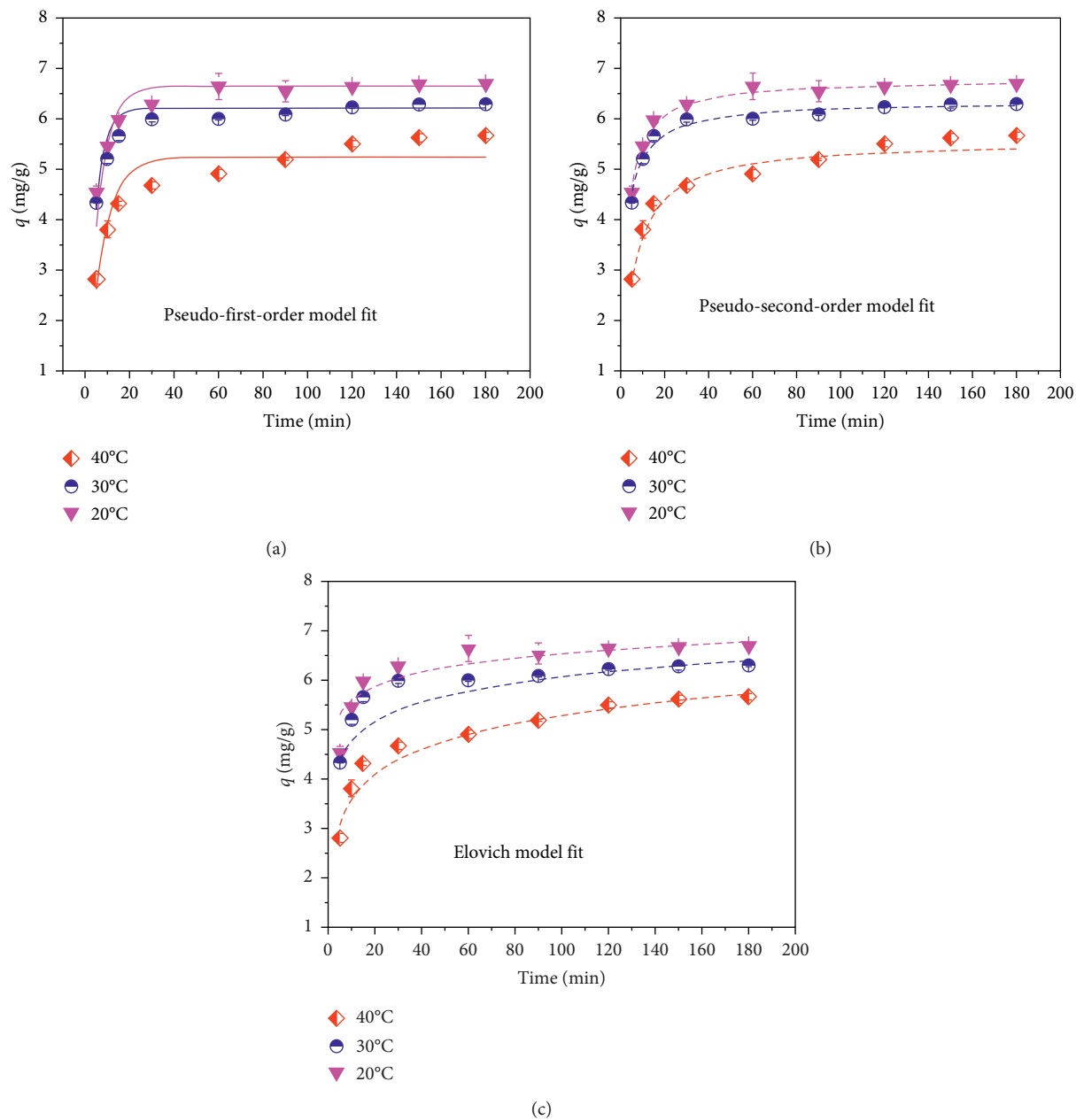


FIGURE 6: Effect of the contact time on Cr(VI) adsorption onto FSS at various temperatures; pH 2; 10 mg/L of initial Cr(VI); 4 g/L of adsorbent dosage.

TABLE 2: The calculated kinetic parameters of Cr(VI) adsorption onto FSS of models at various temperatures.

	Unit	Temperature		
		20°C	30°C	40°C
Pseudo-first-order model				
q_e	mg/g	6.65	6.22	5.24
k_1	1/min	0.174	0.239	0.139
R^2	—	0.920	0.987	0.798
Pseudo-second-order model				
q_e	mg/g	6.78	6.34	5.56
k_2	g/mg × min	0.063	0.068	0.034
R^2	—	0.995	0.997	0.931
Elovich model				
α	mg/g × min	9.853	9.562	9.292
β	mg/g	2.422	1.779	1.348
R^2	—	0.895	0.977	0.963

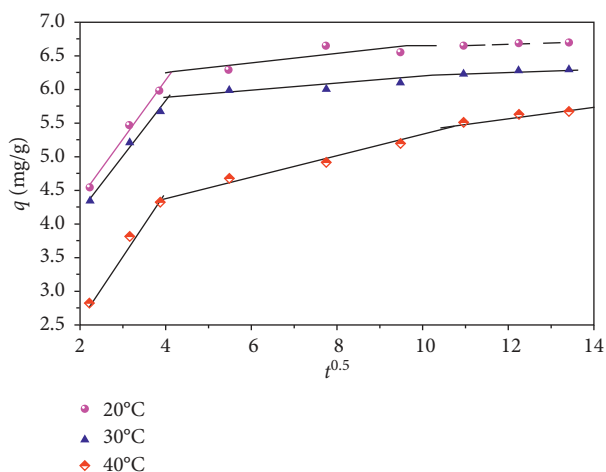


FIGURE 7: Intraparticle diffusion model for Cr(VI) adsorption onto FSS at 20, 30, and 40°C.

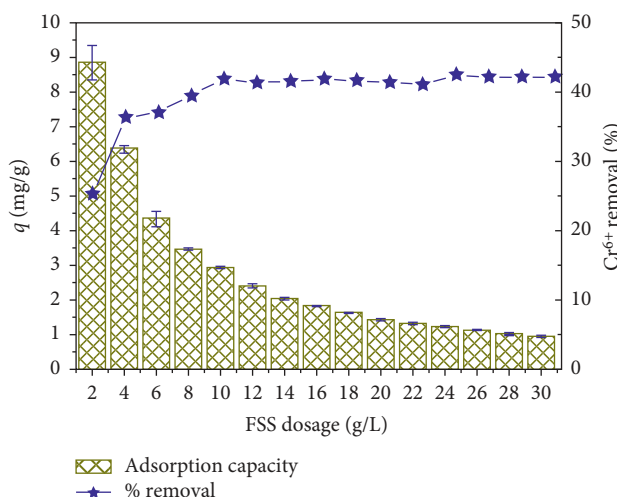


FIGURE 8: Effect of FSS dosage on Cr(VI) adsorption by FSS at 30 mg/L of initial Cr(VI); pH 2; 20°C; 120 min of contact time.

where T is the temperature (K), R is the gas constant (8.314 J/mol K), and K is recalculated from Langmuir constant (K_L) according to the following equation:

$$K = 55.5K_L, \quad (18)$$

where 55.5 is the molar concentration of water. ΔH and ΔS can be determined from the intercept and slope of the plot between $\ln K$ versus $1/T$, respectively. The obtained results are given in Table 3.

The negative enthalpy change (ΔH°) value indicated that the Cr(VI) adsorption onto FSS is an exothermic process. The standard entropy ΔS° was found to be -74.572 J/mol, implying that the randomness at the solid/solution interface decreased during the adsorption process. In general, the values of ΔG° between 0 and -20 kJ/mol indicating the physical adsorption and the chemical adsorption occur when the ΔG° value ranged from -80 to -400 kJ/mol [40]. The Gibbs free energy change values (ΔG°) reached from -6.639

TABLE 3: Thermodynamic parameters for adsorption of Cr(VI) onto FSS.

Temperature (°C)	Thermodynamic parameters		
	ΔG° (kJ/mol)	ΔH° (kJ/mol)	ΔS° (J/mol)
20	-6.639	-28.384	-74.572
30	-5.563	—	—
40	-5.011	—	—

to -5.011 kJ/mol at 20, 30, and 40°C which shows the adsorption process is feasible and spontaneous [26, 40].

4. Conclusion

The shells of freshwater snails (FSSs) are an effective and low-cost biosorbent for removing Cr(VI) from aqueous solutions. The Cr(VI) adsorption process onto FSS was strongly dependent on the solution pH. This study found that adsorption of Cr(VI) onto FSS reached the maximum adsorption capacity at pH 2 in the range of 2–9. The results also showed that the adsorption capacity of Cr(VI) by FSS increased with decreasing the dosage of FSS, initial concentration of Cr(VI), and contact time along with a decrease in temperature from 20 to 40°C. The highest adsorption capacity of Cr(VI) by FSS was 8.85 mg/g in 60 min of contact time with a FSS dose of 2 g/L at 30 mg/L of initial Cr(VI) in this study. The highest Cr(VI) adsorption capacity predicted by Langmuir and Sips, respectively, was 10.69 and 8.91 mg/g at 20°C. The adsorption process occurred spontaneously (ΔG°) and exothermically (ΔH°). The pseudo-second-order model fit best to experimental data of Cr(VI) adsorption onto FSS. The adsorption mechanisms are suggested to be electrostatic interaction and ion exchange. Additionally, the adsorption rate was controlled by film diffusion. It can be concluded that FSS—a food waste that frequently occurs in Vietnam restaurants with solid waste—is a promising low-cost biosorbent for removing Cr(VI) from aqueous solutions.

Data Availability

The data used to support the findings of this study are included within the article.

Conflicts of Interest

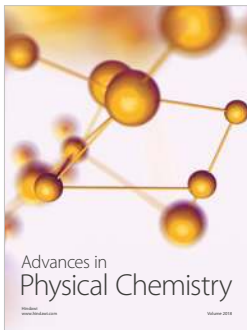
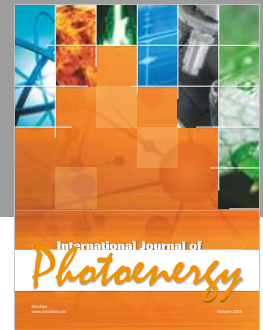
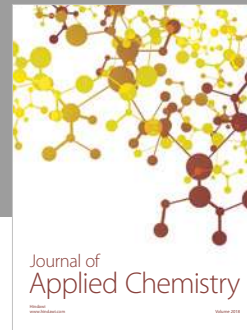
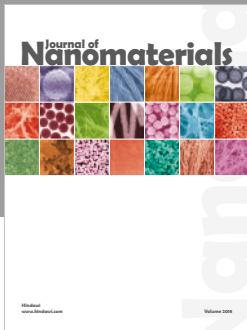
The authors declare no possible conflicts of interest.

References

- [1] K. N. Sheth and V. M. Soni, “Comparative study of removal of CR(VI) with PAC, GAC and adsorbent prepared from tobacco stems,” *Journal of Industrial Pollution Control*, vol. 47, pp. 218–221, 2005.
- [2] K. Selvi, S. Pattabhi, and K. Kadirvelu, “Removal of Cr(VI) from aqueous solution by adsorption onto activated carbon,” *Bioresource Technology*, vol. 80, no. 1, pp. 87–89, 2001.
- [3] S. Kumar and B. C. Meikap, “Removal of chromium(VI) from waste water by using adsorbent prepared from green coconut shell,” *Desalination and Water Treatment*, vol. 52, no. 16–18, pp. 3122–3132, 2014.

- [4] S. K. Singh, "Removal of hexavalent chromium Cr(VI) by using sugarcane bagasse as an low cost adsorbent," *India Journal of Scientific Research*, vol. 13, p. 13, 2017.
- [5] D. Berihun, "Removal of chromium from industrial wastewater by adsorption using coffee husk," *Journal of Material Science and Engineering*, vol. 6, no. 2, pp. 331–340, 2017.
- [6] E. L. Hawley, R. A. Deeb, M. C. Kavanaugh, and R. G. James Jacobs, "Treatment technologies for chromium(VI)," in *Chromium(VI) Handbook*, J. Guertin, J. A. Jacobs, and C. P. Avakian, Eds., CRC Press, Boca Raton, FL, USA, 2004.
- [7] V. Lugo-Lugo, L. A. Bernal-Martínez, F. Ureña-Núñez, I. Linares-Hernández, P. T. Almázán-Sánchez, and P. D. J. B. Vázquez-Santillán, "Treatment of Cr(VI) present in plating wastewater using a Cu/Fe galvanic reactor," *Fuel*, vol. 138, pp. 203–214, 2014.
- [8] Y. B. Xu, H. H. Xiao, and S. Y. Sun, "Study on anaerobic treatment of wastewater containing hexavalent chromium," *Journal of Zhejiang University. Science*, vol. 6B, no. 6, pp. 574–579, 2005.
- [9] J. Qian, L. Wei, R. Liu, F. Jiang, X. Hao, and G.-H. Chen, "An exploratory study on the pathways of Cr(VI) reduction in sulfate-reducing up-flow anaerobic sludge bed (UASB) reactor," *Scientific Reports*, vol. 6, no. 1, pp. 1–12, 2016.
- [10] J. Kanagaraj, N. K. Chandra Babu, and A. B. Mandal, "Recovery and reuse of chromium from chrome tanning waste water aiming towards zero discharge of pollution," *Journal of Cleaner Production*, vol. 16, no. 16, pp. 1807–1813, 2008.
- [11] I. A. Salem, T. A. Fayed, M. N. El-Nahass, and M. Dawood, "A comparative study for adsorption of methylene blue dye from wastewater on to three different types of rice ash," *Journal of Pharmaceutical and Applied Chemistry*, vol. 4, no. 2, pp. 99–107, 2018.
- [12] N. Suganthi, "Removal of chromium(VI) from wastewater using phosphoric acid treated activated carbon," in *Proceedings of the AIP Conference Proceedings*, pp. 128–134, Mumbai, India, June 2013.
- [13] T. C. Machado and M. A. Lansarin, "Wastewater containing Cr(VI) treatment using solar tubular reactor," *Water Science and Technology*, vol. 74, pp. 1698–1705, 2016.
- [14] S. Rao, H. Lade, T. Kadam et al., "Removal of chromium from tannery industry effluents with (activated carbon and fly ash) adsorbents," *Indian Journal of Environmental Health*, vol. 49, pp. 255–258, 2007.
- [15] K. Ait Bentaleb, E. El Khattabi, M. Lakraimi et al., "Removal of Cr(VI) from wastewater by anionic clays," *Journal of Materials and Environmental Science*, vol. 7, pp. 2886–2896, 2016.
- [16] X. M. Dai, S. N. Wang, and X. Wang, "Study on the removal effect of chromium(VI) in wastewater by rice husk," *Advanced Materials Research*, vol. 1073–1076, pp. 825–828, 2015.
- [17] K. M. Al-Qahtani, "Water purification using different waste fruit cortexes for the removal of heavy metals," *Journal of Taibah University for Science*, vol. 10, no. 5, pp. 700–708, 2016.
- [18] M. K. Rai, G. Shahi, V. Meena et al., "Removal of hexavalent chromium Cr(VI) using activated carbon prepared from mango kernel activated with H_3PO_4 ," *Resource-Efficient Technologies*, vol. 2, pp. S63–S70, 2016.
- [19] J. V. Flores-Cano, R. Leyva-Ramos, J. Mendoza-Barron, R. M. Guerrero-Coronado, A. Aragón-Piña, and G. J. Labrada-Delgado, "Sorption mechanism of Cd(II) from water solution onto chicken eggshell," *Applied Surface Science*, vol. 276, pp. 682–690, 2013.
- [20] M. El Haddad, "Removal of Basic Fuchsin dye from water using mussel shell biomass waste as an adsorbent: equilibrium, kinetics, and thermodynamics," *Journal of Taibah University for Science*, vol. 10, no. 5, pp. 664–674, 2016.
- [21] H. T. Van, L. H. Nguyen, V. D. Nguyen et al., "Characteristics and mechanisms of cadmium adsorption onto biogenic aragonite shells-derived biosorbent: batch and column studies," *Journal of Environmental Management*, vol. 241, pp. 535–548, 2018.
- [22] B. Zhao, J. E. Zhang, W. Yan, X. Kang, C. Cheng, and Y. Ouyang, "Removal of cadmium from aqueous solution using waste shells of golden apple snail," *Desalination and Water Treatment*, vol. 57, no. 50, pp. 23987–24003, 2016.
- [23] W. Wu, L. Zhang, Z. Yang, and W. Hou, "Study on the microstructure of the *Pinctada martensii* pearls and its significance," *ISRN Spectroscopy*, vol. 2012, Article ID 756217, 9 pages, 2012.
- [24] J. Balmain, B. Hannoyer, and E. Lopez, "Fourier transform infrared spectroscopy (FTIR) and X-ray diffraction analyses of mineral and organic matrix during heating of mother of pearl (nacre) from the shell of the mollusc *Pinctada maxima*," *Journal of Biomedical Materials Research*, vol. 48, no. 5, pp. 749–754, 1999.
- [25] A. P. Lim and A. Z. Aris, "Continuous fixed-bed column study and adsorption modeling: removal of cadmium (II) and lead (II) ions in aqueous solution by dead calcareous skeletons," *Biochemical Engineering Journal*, vol. 87, pp. 50–61, 2014.
- [26] M. S.-I. Alfa-Sika, F. Liu, and H. Chen, "Optimization of key parameters for chromium (VI) removal from aqueous solutions using activated charcoal," *Journal of Soil Science and Environmental Management*, vol. 1, no. 3, pp. 55–62, 2010.
- [27] M. Akram, H. N. Bhatti, M. Iqbal, S. Noreen, and S. Sadaf, "Biocomposite efficiency for Cr(VI) adsorption: kinetic, equilibrium and thermodynamics studies," *Journal of Environmental Chemical Engineering*, vol. 5, no. 1, pp. 400–411, 2017.
- [28] J. R. Memon, S. Q. Memon, M. I. Bhangar, A. El-Turki, K. R. Hallam, and G. C. Allen, "Banana peel: a green and economical sorbent for the selective removal of Cr(VI) from industrial wastewater," *Colloids and Surfaces B: Biointerfaces*, vol. 70, no. 2, pp. 232–237, 2009.
- [29] S. O. Owalude and A. C. Tella, "Removal of hexavalent chromium from aqueous solutions by adsorption on modified groundnut hull," *Beni-Suef University Journal of Basic and Applied Sciences*, vol. 5, no. 4, pp. 377–388, 2016.
- [30] A. Sdiri, T. Higashi, F. Jamoussi, and S. Bouaziz, "Effects of impurities on the removal of heavy metals by natural limestones in aqueous systems," *Journal of Environmental Management*, vol. 93, no. 1, pp. 245–253, 2012.
- [31] Y.-S. Ho, W.-T. Chiu, and C.-C. Wang, "Regression analysis for the sorption isotherms of basic dyes on sugarcane dust," *Bioresource Technology*, vol. 96, no. 11, pp. 1285–1291, 2005.
- [32] A. Witek-Krowiak, R. G. Szafran, and S. Modelski, "Biosorption of heavy metals from aqueous solutions onto peanut shell as a low-cost biosorbent," *Desalination*, vol. 265, no. 1–3, pp. 126–134, 2011.
- [33] M. A. Hossain, H. H. Ngo, W. S. Guo, and T. V. Nguyen, "Removal of copper from water by adsorption onto banana peel as bioadsorbent," *International Journal of Geomate*, vol. 2, pp. 227–234, 2012.
- [34] I. Langmuir, "The adsorption of gases on plane surfaces of glass, mica and platinum," *Journal of the American Chemical Society*, vol. 40, no. 9, pp. 1361–1403, 1918.
- [35] H. M. F. Freundlich, "Over the adsorption in solution," *Journal of Physical Chemistry*, vol. 57, pp. 370–485, 1906.

- [36] M. Ganesapillai and P. Simha, "The rationale for alternative fertilization: equilibrium isotherm, kinetics and mass transfer analysis for urea-nitrogen adsorption from cow urine," *Resource-Efficient Technologies*, vol. 1, no. 2, pp. 90–97, 2015.
- [37] I. D. L. C. Alomá, I. Rodríguez, M. Calero, and G. Blázquez, "Biosorption of Cr^{6+} from aqueous solution by sugarcane bagasse," *Desalination and Water Treatment*, vol. 52, no. 31–33, pp. 5912–5922, 2014.
- [38] J. Aravind, G. Sudha, P. Kanmani, A. J. Devisri, S. Dhivyalakshmi, and M. Raghavprasad, "Equilibrium and kinetic modeling of chromium (VI) removal from aqueous solution by a novel biosorbent," *Research Journal Of Chemistry And Environment*, vol. 18, pp. 30–36, 2014.
- [39] Q. Manzoor, R. Nadeem, M. Iqbal, R. Saeed, and T. M. Ansari, "Organic acids pretreatment effect on *Rosa bourbonia* phyto-biomass for removal of Pb(II) and Cu(II) from aqueous media," *Bioresource Technology*, vol. 132, pp. 446–452, 2013.
- [40] K. M. Doke and E. M. Khan, "Equilibrium, kinetic and diffusion mechanism of Cr(VI) adsorption onto activated carbon derived from wood apple shell," *Arabian Journal of Chemistry*, vol. 10, pp. S252–S260, 2017.
- [41] Z.-N. Huang, X.-L. Wang, and D.-S. Yang, "Adsorption of Cr(VI) in wastewater using magnetic multi-wall carbon nanotubes," *Water Science and Engineering*, vol. 8, no. 3, pp. 226–232, 2015.
- [42] N. H. Kera, M. Bhaumik, K. Pillay, S. S. Ray, and A. Maity, "Selective removal of toxic Cr(VI) from aqueous solution by adsorption combined with reduction at a magnetic nano-composite surface," *Journal of Colloid and Interface Science*, vol. 503, pp. 214–228, 2017.
- [43] M. Jamshaid Iqbal, F. Cecil, K. Ahmad et al., "Kinetic study of Cr(III) and Cr(VI) biosorption using *rosa damascena* phytomass: a rose waste biomass," *An Asian Journal*, vol. 25, pp. 2099–2103, 2013.
- [44] P. Simha, P. Banwasi, M. Mathew, and M. Ganesapillai, "Adsorptive resource recovery from human urine: system design, parametric considerations and response surface optimization," *Procedia Engineering*, vol. 148, pp. 779–786, 2016.



Hindawi

Submit your manuscripts at
www.hindawi.com

